



Synthesis and Characterization of Iron Oxide Nanoparticles from Coal Fly Ash Waste and their Application for the Removal of Methyl Red Dye from Aqueous Solutions

Virendra Kumar Yadav¹, Nisha Choudhary², Pankaj Kumar^{3*} and M. H. Fulekar⁴

¹Marwadi University Research Center, Department of Microbiology, Faculty of Sciences, Marwadi University, Rajkot, GJ, India

²Department of Life Sciences, Parul Institute of Applied Sciences, Parul University, Vadodara, GJ, India

³Department of Environmental Science, Parul Institute of Applied Sciences, Parul University, Vadodara, GJ, India

⁴Centre for Research for Development, Parul University, Wagodia, Vadodara, GJ, India

Received: 22.09.2024 Accepted: 01.12.2024 Published: 30.12.2024

*pankajb434@yahoo.com



ABSTRACT

Coal fly ash is a major global challenge for human health and the environment. Tremendous efforts have been made to develop value-added materials from coal fly ash (CFA). One such attempt was made in this work to recover crude iron fraction from the CFA by the wet magnetic separation method; the extracted crude iron and concentrated HCl were subjected to sonication and heating to obtain iron leachate. In the first step, iron extracted from CFA was mixed with concentrated HCl, sonicated for 2 hours, and heated at 60 °C. Then, the acidic iron-rich leachate was utilized as a precursor material for forming iron oxides by using NaOH precipitation methods. Then the iron oxide nanoparticles (IONPs) were analyzed using XRD, FT-IR, and FE-SEM techniques. The spherical to cuboidal shape of IONPs of size 80-500 nm was revealed by FE-SEM. The IR showed typical bands at 444, 601, 1101, 1406, 1742, 2007, and 3127 cm⁻¹, while XRD revealed peaks at 31.020° and 44.830° and a small intensity peak at 34.710°, indicating the formation of IONPs. Further, the synthesized IONPs were evaluated for the remediation of methyl red (MR) dye from the simulated wastewater. The adsorption efficiency of MR dye was about 64.75%. Such techniques for utilizing industrial waste for synthesizing value-added materials like IONPs and their application for removing dyes from wastewater make the entire process economical.

Keywords: Fly ash; Methyl red; Iron oxide nanoparticles; Remediation; Transformation.

1. INTRODUCTION

Nanotechnology and nanoparticles (NPs) have played a tremendous role in all fields of science, for instance, research, drug delivery, environmental clean-up, and electronics (Haswani *et al.* 2024; Miao *et al.* 2024; Mehta *et al.* 2024). The drastic increase in the applications of NPs is especially due to the small surface area-to-volume ratio (SVR), high efficiency, and excellent features (Eker *et al.* 2024; Patel *et al.* 2024). Among all the NPs, only a few have gained prominence, such as zinc oxide NPs (Modi *et al.* 2022), alumina NPs, TiO₂ NPs, silica NPs (Nicola *et al.* 2020) and IONPs (Patel *et al.* 2023; Kumar *et al.* 2024). Even though all these NPs have numerous advantages, their expensive synthesis technique, precursor, and characterization make them highly expensive. Due to this, NPs are not the first choice for various research-based investigations. Out of all the metal oxide NPs and magnetic NPs, IONPs have gained huge popularity in recent years due to their advantageous features, ease of manipulation in an external magnetic field, recoverable nature, and low cost (Han *et al.* 2024). Due to all these properties, IONPs are

being widely used in the remediation of pollutants (organic and inorganic), electronics (recording tape, sensors), biomedicine (MRI, drug delivery, hyperthermia), magnetic ink printing, etc. (Rajendran *et al.* 2023; Perwez *et al.* 2023). The suitability and applications of IONPs in all these fields are governed by their size and shape.

It is very important to have a specific size and shape for the IONPs to be used in electronics, magnetic resonance imaging (MRI) (Deeraj C *et al.* 2024; Sun *et al.* 2024), and environmental clean-up. Moreover, the IONPs could exist in amorphous or crystalline phases, deciding their part in further applications.

IONPs are synthesized from iron salt precursors for all these applications, making them expensive. So, there is a need for an economical precursor for the synthesis of IONPs. Several researchers have reported the formation of IONPs from several industrial wastes like red mud (Liu *et al.* 2018), iron scrap, incense stick ash (Gupta *et al.* 2022), and coal fly ash (Li *et al.* 2022). Out of all these industrial wastes, CFA is the most potential candidate due to their high ferrous content (5-

15%) and availability in vast amounts as a waste (Marinina *et al.* 2021). CFA is a heterogeneous material that is generated during the burning of pulverized coal in thermal power plants at the time of generation of electricity (Rafieizonooz *et al.* 2022). Every year, a huge amount of CFA is produced, and the majority of them are left unused, leading to water and soil pollution (Mohebbi *et al.* 2022). Using CFA as a source of ferrous materials could thus prove to be a revolutionary step in the scientific domain.

IONPs of different shapes and sizes have been synthesized by various investigators as per their needs, but rarely any attempt has been made for the form of IONPs from crude iron from CFA (Zanata *et al.* 2022; Sharma *et al.* 2022). So, there is a need to fine-tune the size and shape of IONPs synthesized from wastes like CFA and provide economical IONPs for MRI (Besenhard *et al.* 2021), research, electronics, and environmental applications. The useability of such waste-synthesized IONPs could be enhanced by eliminating their impurities. Previously, Ba-Abbad *et al.* synthesized magnetite NPs of different shapes and sizes using the co-precipitation method and finally applied them to different applications. The investigators used iron precursors to form IONPs (Ba-Abbad *et al.* 2022).

Twinkle *et al.* used iron dust waste (from the steel industry) to synthesize IONPs. The surface area of the magnetically active IONPs was reported to be almost 4.5 times more than that of iron dust (Twinkle *et al.* 2024). Yadav *et al.* (2023) extracted ferrous particles from CFA, which were further treated with acids to obtain the iron leachate. Finally, the investigators obtained IONPs by using the precipitation method. The investigator further assessed the potential of the developed IONPs for the removal of heavy metals (Pb and Cr ions) from CFA aqueous solutions (Yadav *et al.* 2023).

The synthesis of IONPs from CFA involves three sequential steps - the first step involves the extraction of ferrous materials from CFA, followed by acidic treatment of ferrous materials to obtain acidic leachate, and lastly, the precipitation of iron oxides by an alkali. The particle size of the synthesized IONPs varied from 30–70 nm, and purity was about 90–93%, as confirmed by transmission electron microscope (TEM) and electron diffraction spectroscopy (EDS). Further, the synthesized IONPs were used to remediate various heavy metals, especially Pb and Cr ions, from 20% CFA aqueous solutions. The heavy-metal removal efficiency of IONPs varied from 40–70%. The developed method suggests heavy metal removal from wastewater by using an economical and greener route. Each year, a huge number of dyes are produced by the textile industries, which need to be eliminated by an efficient technique like nanotechnology-based adsorption as other approaches

like precipitation (Wang *et al.* 2021), coagulation (Bahrodin *et al.* 2021), filtration (Paixão *et al.* 2024), etc, are less efficient. Moreover, utilizing IONPs as an absorbent from waste will further reduce the removal of dyes from wastewater. Besides this, the IONPs could easily be manipulated by using an external magnetic field and recovered after the completion of the experiment, which will further reduce the cost of the dye elimination from wastewater (Gambhir *et al.* 2022; Tai *et al.* 2023).

In the present research, investigators have extracted iron from CFA using the wet separation method. One of the objectives was to obtain an economical iron precursor by acidic dissolution of iron from CFA, which was accomplished by sonication. Another objective was to synthesize economical IONPs from iron precursors from CFA by using a chemical route, followed by the characterization of the synthesized IONPs for their purity, morphology, and other properties. The final objective was to investigate the efficiency of the IONPs as an adsorbent for the adsorption of methyl red dye from the simulated wastewater. Such approaches will provide an economical solution for pollutant elimination from the environment.

2. MATERIALS AND METHODS

2.1. Materials

Iron particles were recovered from CFA obtained from the Thermal power plant in Gandhinagar, India. Acetic acid and ferrous sulfate heptahydrate were procured from Sigma Aldrich, Germany, concentrated HCl from RANKEM, Gujarat, India, ferric chloride from Merck, India, ethanol from Shenzhen, China, and NaOH pellets from HiMedia, Gujarat, India. All the chemicals were of analytical grade with the highest purity and were used without further purification.

2.2. Methods

2.2.1 Synthesis and Purification of IONPs

The iron from CFA was treated with concentrated HCl under sonication and heating and finally cooled, centrifuged, washed, and collected. The following steps synthesized iron oxides from iron recovered from CFA (Fig. 1).

2.2.2. Preparation of Aqueous Solution of Methyl Red Dye

About 25 mg of methyl red (MR) dye powder granules were added to an amber bottle of 1000 mL double-distilled water to prepare a 25 ppm MR dye stock solution. The dye stock solution was kept on a magnetic stirrer and agitated to dissolve all the dye granules. It was then filtrated using Whatman Filter paper No. 42 to eliminate dirt and impurities. The MR dye stock solution was kept in the amber glass bottle for further application.



Fig. 1: Steps involved in HCl-based extraction of iron and synthesis of IONPs

2.2.3. Batch Study of Adsorption of Methyl Red Dye

About 200 ml of an aqueous solution of MR dye was taken in an Erlenmeyer flask from the stock solution, to which 1 mg IONPs was added. The flask was kept in an orbital shaker at 30 °C at 150 rpm. Further, an aliquot (2-3 ml) was taken out at fixed time intervals - 0, 20, 40, 60, 120, and 180 minutes, and investigated by the UV spectrophotometer for detecting the concentration of MR dye in the sample. The UV-Vis absorbance maxima of MR dye are near 414 nm. Further, the percentage removal of the MR dye by using IONPs was calculated by using the following formula: (1) (Swathilakshmi *et al.* 2022):

$$\text{Dye removal (\%)} = \frac{C_0 - C_t}{C_0} \times 100 \quad \dots (1)$$

Where, C_0 =initial concentration of dye, C_t =concentration of dye at a specific time.

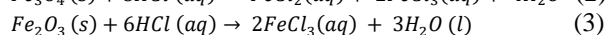
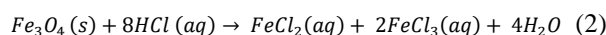
3. CHARACTERIZATION OF THE DEVELOPED IONPS

The identification of the functional groups along with the molecules in the synthesized IONPs was done by using FTIR investigation. The investigation was done using a solid KBr pellet technique where the KBr (89 mg) was mixed thoroughly with IONPs (2 mg) with the help of a mortar pestle. Further, a pellet was prepared by applying the pellet-making machine. The IR investigation of the IONPs was done against a blank sample of KBr in the IR range of 400-4000 cm^{-1} at a resolution of 2 cm^{-1} by S6500 Spectrum instrument (Perkinelmer, USA). The phase identification and crystallinity of the synthesized IONPs were done by using XRD in the 2-theta range of 20-70. The conditions for collecting the XRD pattern were step size = 0.02, time = 5 s per step, voltage = 40 kV, and current = 30 mA. The XRD was collected by investigating the IONP powder

using a D-8 Advanced (Bruker, Netherlands) instrument equipped with an X'celerator. The surface morphological investigation of the developed IONPs was done using FE-SEM, carried out by the Novo Nanosem, FEI 450 (USA). The dried IONPs were loaded on the carbon tape and, in turn, placed on the Al stub holder. The elemental analysis of IONPs was analyzed by an Oxford Electron Dispersive Spectroscopy (EDS) Analyzer fitted with FE-SEM at 20 kV.

4. RESULTS AND DISCUSSION

The CFA iron has mixed phases of iron oxides, for instance, magnetite, maghemite, hematite, and many more elements, which are always present as impurities, as evident from various pieces of literature. Therefore, treatment of iron with concentrated HCl under sonication at 60-70 °C causes the dissolution of iron from crude iron of CFA into the HCl, leading to the formation of aqueous solutions of ferrous and ferric chloride, according to the following reactions:



As Fe has a high solubility in the HCl, a large amount of iron present on the crude iron surface interacts with the acids to form salts of Fe (Valeev *et al.* 2018; Sunjidmaa *et al.* 2019; Baldo *et al.* 2022). During the reactions, the ferrous oxides in CFA are initially impure owing to the presence of Al, Si, C, Ti, Na, etc.; after reacting with acids, they form aqueous ferrous solutions. The crude iron extracted from CFA also has other alkali metals like Mg, Na, Ca, and K, which react with HCl and form chloride salts of respective metals in the leachate.

4.1 Morphological Analysis by FESEM-EDS

The FE-SEM images show that the size of the synthesized IONPs varies from nanometers to microns (Fig. 2a-b). The micrographs show the presence of both cuboidal and spherical particles, but cuboidal particles were dominant. Note: Fig. 2f is adapted with the permission of (Yadav *et al.* 2023). The IONPs show aggregation along with granular white color depositions on their surface. The size of the agglomerated and irregular-shaped particles varies from 300 nm to 1400 nm in diameter. Earlier, Yadav *et al.* (2023) extracted ferrous content from the CFA and synthesized IONPs, which were generally spherical and aggregated together to form a lump. There were two types of particles: spherical-shaped (40 to 70 nm in diameter) and rod-shaped particles (70 nm in length and 10–20 nm in width) (Yadav *et al.* 2023).

Fig. 2c shows the EDS spot of as-synthesized IONPs, while Fig. 2d shows the EDS spectra of the as-synthesized IONPs. The EDS spectrum shows the presence of Fe, O, Al, Na, Cl, and C. The percentage of

Fe was 22.91% (wt. %), O (38.89%), Na (17.05%), Cl (13.7%), C (7.72%) and Al was just 0.08%. The major peaks of Fe and O indicate the formation of IONPs from the crude iron from CFA. The investigation by Yadav *et al.* (2023) obtained peaks for Fe, O, and C, where Fe was

63%, O was 31%, and C was 4%, indicating the high purity of the synthesized IONPs from the CFA. Carbon was present as an impurity whose source was CFA (Yadav *et al.* 2023).

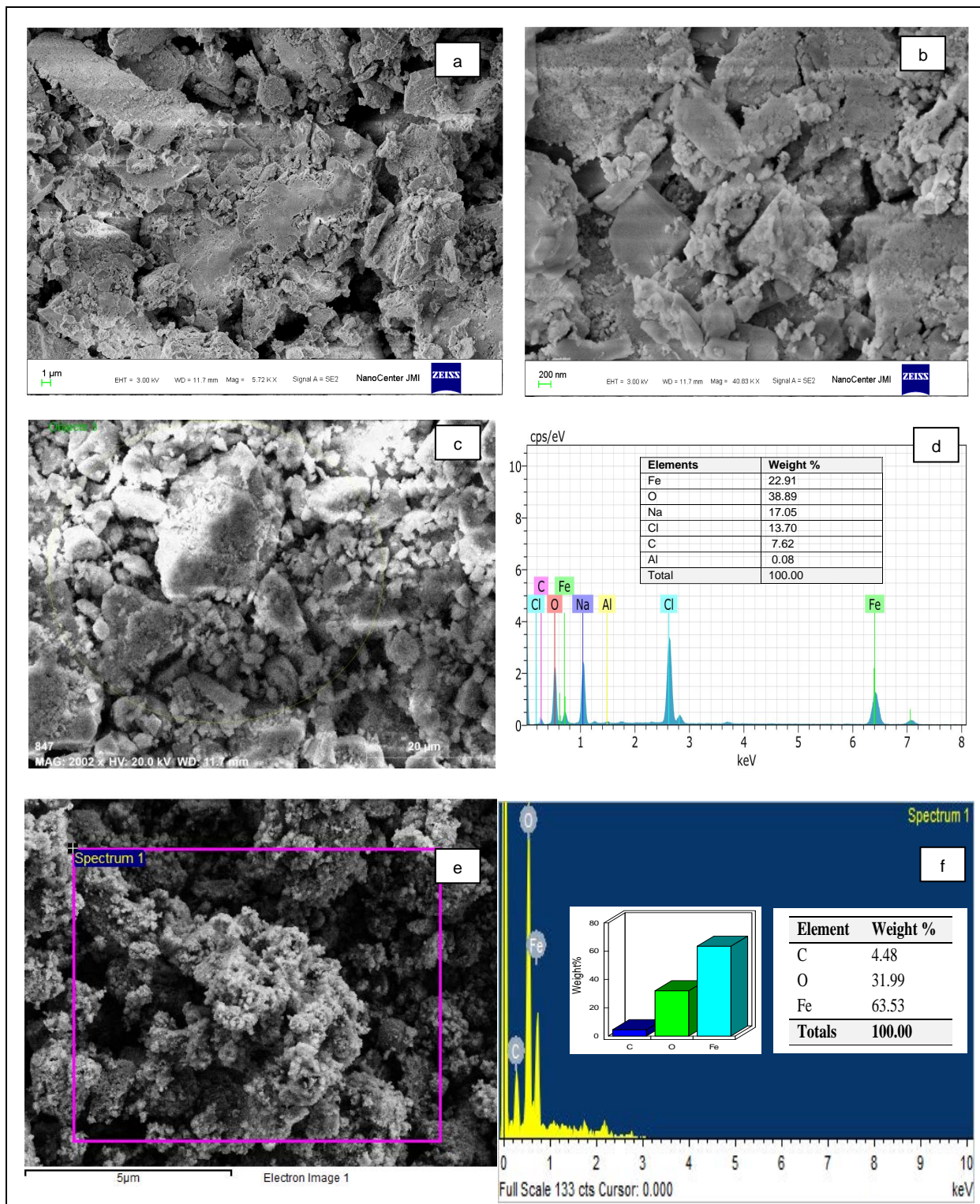


Fig. 2: (a-b) FE-SEM images of as-synthesized IONPs, (c) EDS spot, (d) EDS spectra of as-formed IONPs, and (e-f) EDS spot of purified IONPs and EDS spectra of purified IONPs

The presence of Na and Cl points to the formation of NaCl in the reaction and remains with the IONPs due to improper washing of the IONPs after centrifugation. Al, being amphoteric, was leached out from the crude iron surface during the HCl treatment and presented as an impurity along with the IONPs. However, the Al percentage is just 0.8% in the IONPs. Since crude iron has C in its source, carbon was also present in the iron precursor material, which remained till the formation of IONPs. Fig. 2e shows the EDS spot while Fig. 2f shows EDS spectra of the acetic acid-treated IONPs or purified IONPs, which clearly show peaks for only Fe, O, and C. After purification, Fe was 65.53%, O was 31.53% and C was 4.48% in the IONPs. After purification, all the impurities were eliminated as Na and Al are acid soluble. Moreover, after purification, the percentage of Fe increased threefold while the percentage of carbon and oxygen decreased. The purity of the final IONPs was about 94-96%, suggesting that the treatment with dilute acetic acid is an effective approach for eliminating Na, Cl, and Al from IONPs and other iron sources.

4.2 FTIR Analysis of IONPs for the Identification of Functional Groups

A typical FTIR spectrum of the IONPs synthesized from crude iron from CFA is shown in Fig. 3. The spectrum exhibits characteristic bands at 601, 1101, 1406, 1742, 2007, and 3127 cm^{-1} for the developed IONPs. The band at 601 cm^{-1} was assigned to the bending vibrations of the Fe-O bond, while the band at 1101 cm^{-1} was assigned to the hydrous ferric oxides. A sharp band at 1410 cm^{-1} could be assigned to the C=O/C-H bond. Broadband with its center at 3135 cm^{-1} was attributed to the -OH molecule in the sample as ferric hydroxide. It has two weak bands at its shoulder around 3032 cm^{-1} and 2807 cm^{-1} , which were assigned to the C-H group (Haile *et al.* 2015; González *et al.* 2017; Patel *et al.* 2023). The FTIR confirmed the development of IONPs from the iron precursors obtained from crude iron of CFA. Earlier Yadav *et al.* (2023) obtained bands at 422 cm^{-1} and 576 cm^{-1} , attributed to the vibrational modes of Fe-/Fe-O-Fe (magnetite and maghemite) of IONPs; bands obtained at 3400 cm^{-1} and 1600 cm^{-1} , indicated the presence of OH groups of either water molecules or ferric hydroxides (Fe-O-OH) (Yadav *et al.* 2023).

4.3 Phase Identification of IONPs by XRD

A typical XRD pattern of the IONPs synthesized from crude iron of CFA is shown in Fig. 4. The XRD pattern exhibits two strong intensity peaks at 31.02° and 44.83°, which were associated with the IONPs (Acisli *et al.* 2017). Besides this, there are two small peaks, one at 27.70° and another at 34.71°, indicating quartz and magnetite phases, respectively. The absence of other major peaks from the sample indicates the purity of the developed IONPs. The pattern was matched with PDF No. 03-0746 for IONPs. The XRD

pattern of purified IONPs exhibits the amorphous phase where the broad hump starts at the 2-theta range of 30° and ends at 40°. After purification, the crystallinity of the IONPs is lost (Mahapatra *et al.* 2013; Yadav *et al.* 2020; Yang *et al.* 2023; Kgosiemang *et al.* 2023). Similar results were also obtained by Alshammari *et al.* for the IONPs, whose major peaks were at 27, 29, and 36° (Alshammari *et al.* 2020). Previously, Yadav *et al.* (2020) obtained small intensity peaks for the IONPs synthesized from CFA-extracted ferrous content at 33° and 35°, which are assigned to the hematite and magnetite, respectively (Yadav *et al.* 2023).

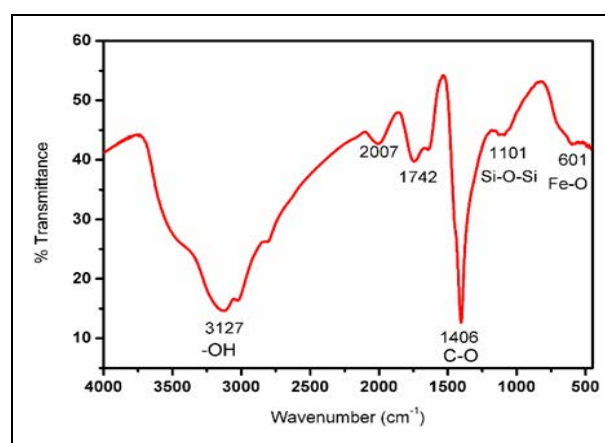


Fig. 3: FTIR spectra of IONPs synthesized from CFA

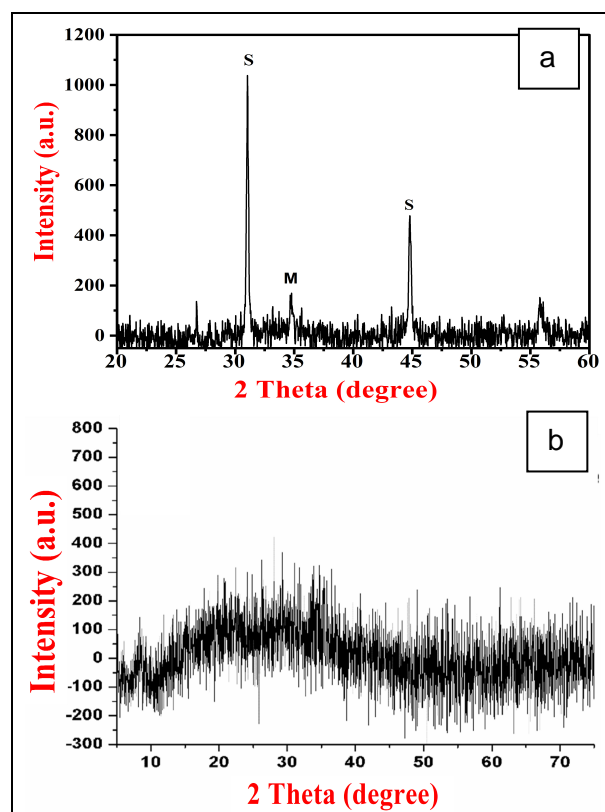


Fig. 4: XRD Diffractograms of IONPs: (a) as synthesized and (b) after purification

4.4. Batch Adsorption Study of Methyl Red Dye by IONPs

MR dye exhibits the highest absorbance at 414 nm when examined using a UV-Vis spectrophotometer (Patil *et al.* 2016; Jusoh N. *et al.* 2017; Amari *et al.* 2023). The UV-Vis spectra of the dye absorbance showed that the concentration of the MR dye continuously decreased from 0 to 180 minutes. The highest concentration of the MR dye was at 0 minutes, while the lower value was reached after 180 minutes, as depicted in Fig. 5. The percentage removal of MR dye was calculated at different time intervals: at the start, there was no removal of MR dye, while at 20 minutes, the removal was 8.3%, which increased to 17.81% at 40 minutes; at 60 minutes, the removal percentage reached to 26.95% while at 120 minutes it was 31.82%, and finally, after 180 minutes, the MR dye removal reached 64.75%. The graph shows that the MR dye removal percentage increased continuously with an increase in the contact time, reaching its maximum at 180 minutes (Fig. 6).

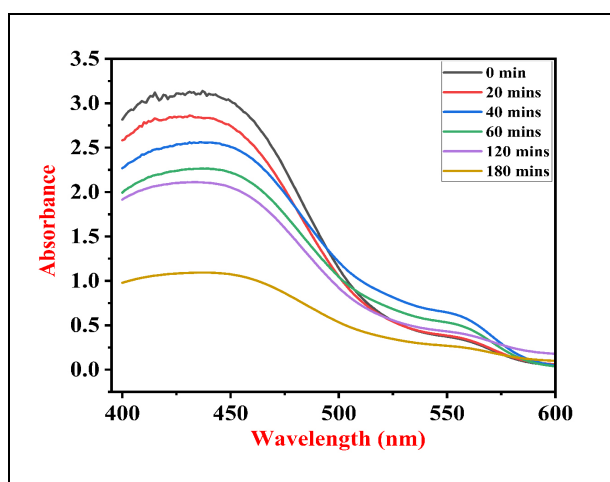


Fig. 5: UV-Vis's spectra of MR dye at different time intervals

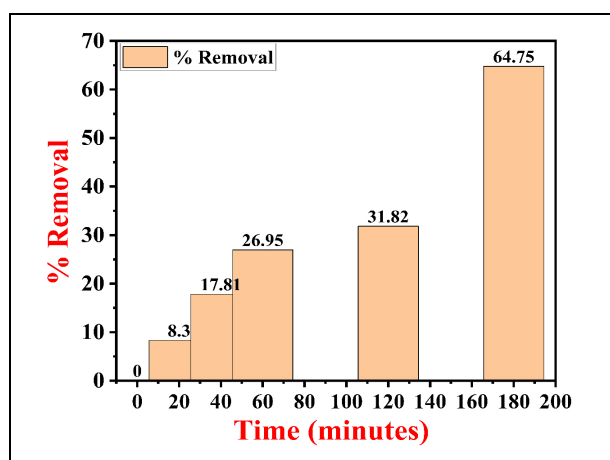


Fig. 6: Percentage removal of MR dye by IONPs

Earlier, twinkle *et al.* developed IONPs, which had an active multiphase of iron oxides ($\text{Fe@Fe}_3\text{O}_4\text{@Fe}_2\text{O}_3$), better mesoporosity, and almost 4.5 times higher surface area than the iron dust waste. Due to these superior features, IONPs were used for the efficient removal of organic dyes, namely Reactive Green 19, Reactive Orange 16, and Malachite Green dye, with the highest removal efficiency of ~ 2162.9 , ~ 2273.1 and ~ 1400.2 mg/g, respectively. Further, the investigation of dyes was related to kinetics, isotherms, and adsorption thermodynamics to understand the mechanism of dye removal. Moreover, the removal of dyes was also assessed against temperature, pH, loading, and concentration (Twinkle *et al.* 2024). Table 1 summarizes the methyl red dye removal by IONPs in the present and previous studies.

Table 1. Removal of methyl red dye by IONPs in the present and previous studies

Types of IONPs	Removal Efficiency	Time (minutes)	References
Nanorods	62.5%	NS	(Rather and Sundarapandian 2024)
Fe_2O_3	94%	90	(Jadhav <i>et al.</i> 2024)
IONPs composites	$\sim 99\%$	NS	(Singh <i>et al.</i> 2022)
Fe NPs	Higher than Cu NPs	NS	(Majadleh <i>et al.</i> 2022)
$\alpha\text{-Fe}_2\text{O}_3$	Effective	NS	(Bhattarai <i>et al.</i> 2023)
Fe_3O_4 NPs	98.61%	180	(Gritli <i>et al.</i> 2024)
IONPs	64.75%	180	Current investigation

5. CONCLUSION

The study exhibits an effective and sustainable approach for synthesizing iron oxide nanoparticles from coal fly ash, which provides an economical solution for environmental remediation. The iron extracted from CFA was associated with the elemental impurities of Al, Si, Na, Mg, Ca, K, P, S, and C, the precursor materials for synthesizing IONPS. The concentrated HCl treatment of iron leached out easily soluble iron from the crude iron into the acidic medium. The IONPs were synthesized from the ferrous leachate by chemical co-precipitation method, with more than 90% purity. The IONPs were cuboidal- to spherical-shaped, with sizes 10-20 nm for spherical and 30-40 nm for cuboidal/rods, as revealed by FE-SEM. The removal efficiency of the MR dye was 64.75% after three hours by the CFA-synthesized IONPs. This method utilizes industrial waste and contributes to wastewater treatment, making it a promising solution for reducing environmental pollutants. The developed techniques can successfully extract the ferrous content that can be used further to synthesize iron oxide nanoparticles in their purest form.

ACKNOWLEDGMENTS

The authors acknowledge the support provided by Marwadi University, Gujarat, India for carrying out this study.

FUNDING

This research received no specific grant from any funding agency in the public, commercial, or not-for-profit sectors.

CONFLICTS OF INTEREST

The authors declare that there is no conflict of interest.

COPYRIGHT

This article is an open-access article distributed under the terms and conditions of the Creative Commons Attribution (CC BY) license (<http://creativecommons.org/licenses/by/4.0/>).



REFERENCES

- Acisli, O., Khataee, A., Darvishi Cheshmeh Soltani, R. and Karaca, S., Ultrasound-assisted Fenton process using siderite nanoparticles prepared via planetary ball milling for removal of reactive yellow 81 in aqueous phase, *Ultrason. Sonochem.*, 35210–218 (2017).
<https://doi.org/10.1016/j.ultsonch.2016.09.020>
- Alshammari, M., Al Juboury, M.F., Naji, L. A., Faisal, A.A.H., Zhu, H., Al-Ansari, N. and Naushad, M., Synthesis of a Novel Composite Sorbent Coated with Siderite Nanoparticles and its Application for Remediation of Water Contaminated with Congo Red Dye, *Int. J. Environ. Res.*, 14(2), 177–191 (2020).
<https://doi.org/10.1007/s41742-020-00245-6>
- Amari, A., Yadav, V. K., Pathan, S. K., Singh, B., Osman, H., Choudhary, N., Khedher, K. M. and Basnet, A., Remediation of Methyl Red Dye from Aqueous Solutions by Using Biosorbents Developed from Floral Waste, *Adsorpt. Sci. Technol.*, 20231532660 (2023).
<https://doi.org/10.1155/2023/1532660>
- Ba-Abbad, M. M., Benamour, A., Ewis, D., Mohammad, A. W. and Mahmoudi, E., Synthesis of Fe₃O₄ Nanoparticles with Different Shapes Through a Co-Precipitation Method and Their Application, *JOM*, 74(9), 3531–3539 (2022).
<https://doi.org/10.1007/s11837-022-05380-3>
- Bahrodin, M. B., Zaidi, N.S., Hussein, N., Sillanpää, M., Prasetyo, D. D. and Syafiuddin, A., Recent Advances on Coagulation-Based Treatment of Wastewater: Transition from Chemical to Natural Coagulant, *Curr. Pollut. Rep.*, 7(3), 379–391 (2021).
<https://doi.org/10.1007/s40726-021-00191-7>
- Baldo, C., Ito, A., Krom, M. D., Li, W., Jones, T., Drake, N., Ignatyev, K., Davidson, N. and Shi, Z., Iron from coal combustion particles dissolves much faster than mineral dust under simulated atmospheric acidic conditions, *Atmospheric Chem. Phys.*, 22(9), 6045–6066 (2022).
<https://doi.org/10.5194/acp-22-6045-2022>
- Besenhard, M. O., Panariello, L., Kiefer, C., LaGrow, A. P., Storozhuk, L., Perton, F., Begin, S., Mertz, D., Thanh, N. T. K. and Gavriilidis, A., Small iron oxide nanoparticles as MRI T₁ contrast agent: scalable inexpensive water-based synthesis using a flow reactor, *Nanoscale*, 13(19), 8795–8805 (2021).
<https://doi.org/10.1039/D1NR00877C>
- Bhattacharai, M. K., Ashie, M. D., Dugu, S., Subedi, K., Bastakoti, B. P., Morell, G. and Katiyar, R. S., Block Copolymer-Assisted Synthesis of Iron Oxide Nanoparticles for Effective Removal of Congo Red, *Molecules*, 28(4), (2023).
<https://doi.org/10.3390/molecules28041914>
- Deeraj C., Subburaj T., and Santhosh S. V., Brain Stroke Detection using Magnetic Resonance Imaging, *Int. J. Adv. Res. Sci. Commun. Technol.*, 63–66 (2024).
<https://doi.org/10.48175/IJARST-19013>
- Eker, F., Duman, H., Akdaşçi, E., Bolat, E., Sarıtaş, S., Karav, S. and Witkowska, A.M., A Comprehensive Review of Nanoparticles: From Classification to Application and Toxicity, *Molecules*, 29(15), 3482 (2024).
<https://doi.org/10.3390/molecules29153482>
- Gambhir, R. P., Rohiwal, S.S. and Tiwari, A.P., Multifunctional surface functionalized magnetic iron oxide nanoparticles for biomedical applications: A review, *Appl. Surf. Sci. Adv.*, 11100303 (2022).
<https://doi.org/10.1016/j.apsadv.2022.100303>
- González, M. A., López, G. M. M., Vereda, A. E., García, D., Torres, A. and Pavón, J. M. C., Development of a new FT-IR method for the determination of iron oxide. Optimization of the synthesis of suitable magnetic nanoparticles as sorbent in magnetic solid phase extraction, *New J. Chem.*, 41(17), 8804–8811 (2017).
<https://doi.org/10.1039/C7NJ01522D>
- Gritli, I., Chemingui, H., Djebali, K., Mabrouk, W., Hafiane, A., Marzouki, R., Ammar, S., Chtourou, R. and Keshk, S. M. A. S., Methylene Blue Adsorption by Fe₃O₄ Nanoparticles: An Optimization Study Using Response Surface Methodology, *Chem. Eng. Technol.*, 47 (2024).
<https://doi.org/10.1002/ceat.202400006>

- Gupta, N., Yadav, V. K., Yadav, K. K., Alwetaishi, M., Gnanamoorthy, G., Singh, B., Jeon, B. H., Cabral-Pinto, M. M. S., Choudhary, N., Ali, D. and Nejad, Z. D., Recovery of iron nano minerals from sacred incense sticks ash waste collected from temples collected from temples by wet and dry magnetic separation method, *Environ. Technol. Innov.*, 25, 102150 (2022).
<https://doi.org/10.1016/j.eti.2021.102150>
- Haile, H. L., Abi, T. and Tesfahun, K., Synthesis, characterization and photocatalytic activity of MnO₂/Al₂O₃/Fe₂O₃ nanocomposite for degradation of malachite green, *Afr. J. Pure Appl. Chem.*, 9(11), 211–222 (2015).
<https://doi.org/10.5897/AJPAC2015.0656>
- Han, B., Zhao, Y., Ma, L., Chen, L., Hou, W., Li, B., Wang, J., Yu, J., Wang, G., He, Y., Ma, M., Zhou, J., Sun, S., Yu, C. and Pan, J., A Minimalist Iron Oxide Nanoprobe for the High-Resolution Depiction of Stroke by Susceptibility-Weighted Imaging, *Small*, 20(44), 2401061 (2024).
<https://doi.org/10.1002/sml.202401061>
- Haswani, A., Torremocha, V. and Lilova, K., Nanotechnology for Neurological Disorders: Application of Nanotechnology in Diagnosing and Treating Neurodegenerative Diseases, *J. Stud. Res.*, 13(2), (2024).
<https://doi.org/10.47611/jsrhs.v13i2.6775>
- Jadhav, A., Chavan, R., Sonawane, S., Kamble, P., Mahajan, S., Vhankhande, B., Ghorpade, R., Chougale, A., Abd El-Salam, N. M., Fouad, H. and Patil, R., *J. Nanoelectron. Optoelectron.*, 19(3), 272–277 (2024).
<https://doi.org/10.1166/jno.2024.3571>
- Jusoh N., Ruseli S. N. N. M., Badri M. F., Husin N. and Hitam S. M. S., Biodecolourization of methyl red dye by bacterial-fungal consortium, *Chem. Eng. Trans.*, 56, 1537–1542 (2017).
<https://doi.org/10.3303/CET1756257>
- Kgosiemang, I. K. R., Adegoke, A. M., Mashele, S. S. and Sekhoacha, M. P., Green synthesis of Iron oxide and Iron dioxide nanoparticles using *Euphorbia tirucalli*: characterization and antiproliferative evaluation against three breast cancer cell lines, *J. Exp. Nanosci.*, 18(1), 2276276 (2023).
<https://doi.org/10.1080/17458080.2023.2276276>
- Li, X., Ma, B., Wang, C., Chen, Y., Yang, W. and Zhang, W., A sustainable process to recycle aluminum from coal fly ash for simultaneous removal of iron: Solid waste management and evaluation, *Miner. Eng.*, 184107638 (2022).
<https://doi.org/10.1016/j.mineng.2022.107638>
- Liu, C., Ma, S., Zheng, S., Luo, Y., Ding, J., Wang, X. and Zhang, Y., Combined treatment of red mud and coal fly ash by a hydro-chemical process, *Hydrometallurgy*, 175224–231 (2018).
<https://doi.org/10.1016/j.hydromet.2017.11.005>
- Mahapatra, A., Mishra, B. G. and Hota, G., Adsorptive removal of Congo red dye from wastewater by mixed iron oxide–alumina nanocomposites, *Ceram. Int.*, 39(5), 5443–5451 (2013).
<https://doi.org/10.1016/j.ceramint.2012.12.052>
- Majadleh, M., Shahwan, T., Ahmed, R. B. and Anjass, M., Application of Fe and Cu nanoparticles for methyl orange removal from water and water-ethanol mixtures under various experimental conditions, *Water Resour. Ind.*, 28, (2022).
<https://doi.org/10.1016/j.wri.2022.100189>
- Marinina, O., Nevskaya, M., Jonek-Kowalska, I., Wolniak, R. and Marinin, M., Recycling of Coal Fly Ash as an Example of an Efficient Circular Economy: A Stakeholder Approach, *Energies*, 14(12), 3597 (2021).
<https://doi.org/10.3390/en14123597>
- Mehta, S., Thakur, A., Kurbah, I., Chauhan, N. and Thakur, R., Nanotechnology in plant nutrition: Ensuring sustainable agriculture through nanofertilizers, *J. Plant Nutr. Soil Sci.*, 187(5), 589–603 (2024).
<https://doi.org/10.1002/jpln.202300288>
- Miao, K., Xia, X., Zou, Y. and Shi, B., Small Scale, Big Impact: Nanotechnology-Enhanced Drug Delivery for Brain Diseases, *Mol. Pharm.*, 21(8), 3777–3799 (2024).
<https://doi.org/10.1021/acs.molpharmaceut.4c00387>
- Modi, S., Yadav, V. K., Gacem, A., Ali, I. H., Dave, D., Khan, S. H., Yadav, K. K., Rather, S., Ahn, Y., Son, C. T. and Jeon, B. H., Recent and Emerging Trends in Remediation of Methylene Blue Dye from Wastewater by Using Zinc Oxide Nanoparticles, *Water*, 14(11), 1749 (2022).
<https://doi.org/10.3390/w14111749>
- Mohebbi, M., Rajabipour, F. and Madadian, E., A framework for identifying the host phases in Coal-derived fly ash, *Fuel*, 314, 122806 (2022).
<https://doi.org/10.1016/j.fuel.2021.122806>
- Nicola, R., Costișor, O., Ciopec, M., Negrea, A., Lazău, R., Ianăși, C., Picioruș, E. M., Len, A., Almásy, L., Szerb, E.I. and Putz, A.-M., Silica-Coated Magnetic Nanocomposites for Pb²⁺ Removal from Aqueous Solution, *Appl. Sci.*, 10(8), 2726 (2020).
<https://doi.org/10.3390/app10082726>
- Paixão, R. M., Silva, L. H. B. R. D., Vieira, M. F., Amorim, M. T. P. D., Bergamasco, R. and Vieira, A. M. S., Enhanced filtration membranes with graphene oxide and tannic acid for textile industry wastewater dye removal, *Environ. Technol.*, 45(1), 1–12 (2024).
<https://doi.org/10.1080/09593330.2024.2369733>
- Patel, D., Patel, B., Yadav, V. K., Sudhakar, M. P., Alharbi, S. A., Salmen, S. H., Patel, I., Choudhary, N. and Patel, A., Silver nanoparticles synthesized from marine algae *Spatoglossum asperum*: Antioxidant properties and seed germination enhancement, *J. Hazard. Mater. Adv.*, 16, 100478 (2024).
<https://doi.org/10.1016/j.hazadv.2024.100478>

- Patel, S., Desai, R., Patel, B., Ali, D., Dawane, V., Gadhvi, K., Yadav, V.K., Choudhary, N., Sahoo, D. K. and Patel, A., Phytanofabrication of iron oxide particles from the *Acacia jacquemontii* plant and their potential application for the removal of brilliant green and Congo red dye from wastewater, *Front. Bioeng. Biotechnol.*, 11, 1319927 (2023). <https://doi.org/10.3389/fbioe.2023.1319927>
- Patil, N., Bholay, A., Kapadnis, B. and Gaikwad, V., Biodegradation of Model Azo Dye Methyl Red and other Textile Dyes by Isolate *Bacillus circulans* NPP1, *J. Pure Appl. Microbiol.*, 10(4), 2793–2800 (2016). <https://doi.org/10.22207/JPAM.10.4.38>
- Perwez, M., Fatima, H., Arshad, M., Meena, V. K. and Ahmad, B., Magnetic iron oxide nanosorbents effective in dye removal, *Int. J. Environ. Sci. Technol.*, 20(5), 5697–5714 (2023). <https://doi.org/10.1007/s13762-022-04003-3>
- Rafieizonooz, M., Khankhaje, E. and Rezanian, S., Assessment of environmental and chemical properties of coal ashes including fly ash and bottom ash, and coal ash concrete, *J. Build. Eng.*, 49, 104040 (2022). <https://doi.org/10.1016/j.jobbe.2022.104040>
- Rajendran, S., Wanale, S.G., Gacem, A., Yadav, V. K., Ahmed, I. A., Algethami, J. S., Kakodiya, S. D., Modi, T., Alsuhaibani, A. M., Yadav, K. K. and Cavalu, S., Nanostructured Iron Oxides: Structural, Optical, Magnetic, and Adsorption Characteristics for Cleaning Industrial Effluents, *Crystals*, 13(3), 472 (2023). <https://doi.org/10.3390/cryst13030472>
- Rather, M. Y. and Sundarapandian, S., Utilization of Eco-friendly Copper Oxide Nanoparticles and Iron Oxide Nanorods in Dye Removal from Real Textile Industry Effluent, *Part. Part. Syst. Charact.*, 41, 2300223 (2024). <https://doi.org/10.1002/ppsc.202300223>
- Sharma, B., Kumari, N., Mathur, S. and Sharma, V., Kinetics and Optimization of Azo Dye Decolorisation Using Green Synthesized Iron-Oxide Nanoparticles: A Pilot Scale Study, *Int. J. Environ. Res.*, 16(4), 38 (2022). <https://doi.org/10.1007/s41742-022-00418-5>
- Singh, N. J., Wareppam, B., Kumar, A., Singh, K. P., Garg, V. K., Oliveira A. C. and Singh H. L., Zeolite incorporated iron oxide nanoparticle composites for enhanced congo red dye removal, *J. Mater. Res.*, 38, 1149–1161 (2023). <https://doi.org/10.1557/s43578-022-00859-w>
- Sun, X., Badachhape, A., Bhandari, P., Chin, J., Annapragada, A. and Tanifum, E., A dual target molecular magnetic resonance imaging probe for noninvasive profiling of pathologic alpha-synuclein and microgliosis in a mouse model of Parkinson's disease, *Front. Neurosci.*, 181, 428736 (2024). <https://doi.org/10.3389/fnins.2024.1428736>
- Sunjidmaa, D., Batdemberel, G. and Takibai, S., A Study of Ferrospheres in the Coal Fly Ash, *Open J. Appl. Sci.*, 09(01), 10–16 (2019). <https://doi.org/10.4236/ojapps.2019.91002>
- Swathilakshmi, A. V., Abirami, S., Geethamala, G. V., Poonkothai, M., Sudhakar, C., Albasher, G., Alamri, O. and Alsultan, N., Phytanofabrication of copper oxide mediated by *Albizia amara* and its photocatalytic efficacy, *Mater. Lett.*, 314, 131911 (2022). <https://doi.org/10.1016/j.matlet.2022.131911>
- Tai, V. C., Che, H. X., Kong, X. Y., Ho, K. C. and Ng, W. M., Decoding iron oxide nanoparticles from design and development to real world application in water remediation, *J. Ind. Eng. Chem.*, 12782–100 (2023). <https://doi.org/10.1016/j.jiec.2023.07.038>
- Twinkle., Tewatia, H., Kaushik, J., Sahu, A., Chaudhary, S.K. and Sonkar, S.K., Waste Iron Dust Derived Iron Oxide Nanoparticles for Efficient Adsorption of Multiple Azo Dyes, *ACS Sustain. Resour. Manag.*, 1(2), 278–288 (2024). <https://doi.org/10.1021/acssusresmg.3c00064>
- Valeev, D., Mikhailova, A. and Atmadzhidi, A., Kinetics of Iron Extraction from Coal Fly Ash by Hydrochloric Acid Leaching, *Metals*, 8(7), 533 (2018). <https://doi.org/10.3390/met8070533>
- Wang, L. K., Wang, M. H. S., Shammam, N. K. and Hahn, H. H., Physicochemical Treatment Consisting of Chemical Coagulation, Precipitation, Sedimentation, and Flotation, In: Wang L. K, Wang M. H. S., Hung Y. T., *Integrated Natural Resources Research, Springer International Publishing, Cham*, 22, 265–397 (2021). https://doi.org/10.1007/978-3-030-61002-9_6
- Yadav, V. K., Amari, A., Gacem, A., Elboughdiri, N., Eltayeb, L. B. and Fulekar, M. H., Treatment of Fly-Ash-Contaminated Wastewater Loaded with Heavy Metals by Using Fly-Ash-Synthesized Iron Oxide Nanoparticles, *Water*, 15(5), 908 (2023). <https://doi.org/10.3390/w15050908>
- Yadav, V. K. and Fulekar, M. H., Advances in Methods for Recovery of Ferrous, Alumina, and Silica Nanoparticles from Fly Ash Waste, *Ceramics*, 3(3), 384–420 (2020). <https://doi.org/10.3390/ceramics3030034>
- Yang, Q., Li, Y., Zhao, X., Zhang, J., Cheng, X. and Zhu, N., Recent advances of superparamagnetic iron oxide nanoparticles and its applications in neuroscience under external magnetic field, *Appl. Nanosci.*, 13(8), 5489–5500 (2023). <https://doi.org/10.1007/s13204-023-02803-8>
- Zanata, L., Tofanello, A., Martinho, H. S., Souza, J. A. and Rosa, D. S., Iron oxide nanoparticles–cellulose: a comprehensive insight on nanoclusters formation, *J. Mater. Sci.*, 57(1), 324–335 (2022). <https://doi.org/10.1007/s10853-021-06564-z>